DOI: 10.1002/ejic.201100352

Syntheses, Structures and Reactivity of New Intramolecularly Coordinated Tin Alkoxides Based on an Enantiopure Ephedrine Derivative

Ljuba Iovkova-Berends,[a] Thorsten Berends,[a] Christina Dietz,[a] Gerrit Bradtmöller,[a] Dieter Schollmeyer,[b] and Klaus Jurkschat*[a]

Keywords: Tin / Alkoxide complexes / NMR spectroscopy / Ephedrine / X-ray diffraction analysis

The syntheses of the tin compounds $[LSn]_2$ (**2**), *spiro*-L_2Sn (**3**), $[LSnW(CO)_5]_2$ (**4**), $[LSnBr_2]_2$ (**5**), *spiro*-$L_2Sn{\cdot}SnBr_4$ (**6**) and $LSn[OC(O)Ph]_2$ (**8**), where L = $MeN(CH_2CMe_2O)[(S)\text{-}CH(Me)\text{-}(R)\text{-}CH(Ph)O]$, and $(Ph_4P)_2SnBr_6$ (**7**) are reported. The compounds were characterized by elemental analysis, multinuclear NMR spectroscopy including ^{119}Sn cross polarisation–magic angle spinning NMR (CP–MAS) (**2**, **3**–**6**), electrospray ionization mass spectrometry (**2**–**4**) and single crystal X-ray diffraction analysis (**2**, **2**·C_7H_8, **3a**, **3b**, **4**·C_7H_8, **5**, **6**·C_7H_8, **7**).

Introduction

In recent years there has been a renewed interest in the chemistry of both tin(II) and tin(IV) derivatives of alkanol amines and related substituted alcohols.[1] The motivation behind these activities stems from academic curiosity into the enormous structural diversity that these compounds exhibit and from their catalytic activity in, for instance, polyurethane formation[2] and ring opening polymerization.[3]

Catalytic activity immediately poses the question of stereoselective transformations, which in turn requires the synthesis of chiral catalysts. In general, transition and main group metal alkoxides of groups 4 and 14 are not stable configurationally. Consequently, chirality can be introduced by the organic backbone of the alkoxide substituent.

In this respect, ephedrine and its derivatives have attracted much attention and an excellent overview of metal complexes of this functionalized alcohol has recently been published.[4] To the best of our knowledge, there is only one ephedrine-based tin compound reported in the literature.[5]

In the context of our ongoing interest in the tin derivatives of ethanol amines[6] we report here a series of ephedrine-derived derivatives.

Results and Discussion

The reaction of the enantiopure ephedrine-derivatized dialkanolamine $MeN(CH_2CMe_2OH)[(\boldsymbol{S})\text{-}CH(Me)\text{-}(\boldsymbol{R})\text{-}CH(Ph)OH]$ (**1**) with the in situ generated tin(II) butoxide in toluene gave a crude reaction mixture, which showed a major broad resonance at δ –243 and a minor intense sharp signal at δ –448 in the ^{119}Sn NMR spectrum (Scheme 1). From this reaction mixture the stanna(II)bicyclooctane **2**, as its toluene solvate **2**·C_7H_8, was isolated as a colourless crystalline material. Recrystallization of **2**·C_7H_8 from a donor solvent (pyridine, nBu_2O, thf, hmpa) gave solvate-free **2** as colourless crystals, which showed a significantly higher melting point than that of **2**·C_7H_8. Both **2**·C_7H_8 and **2** are soluble in polar organic solvents such as CH_2Cl_2, nBu_2O, thf and pyridine.

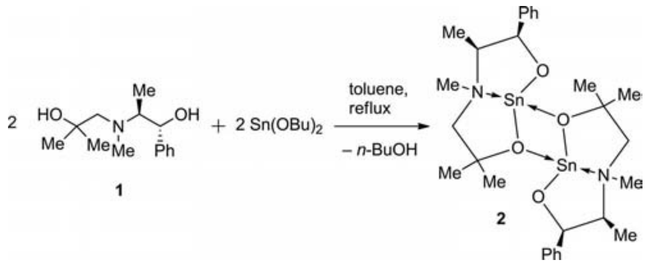

Scheme 1. Synthesis of **2**.

The molecular structure of **2**·C_7H_8, as determined by single-crystal X-ray diffraction analysis, is shown in Figure 1 and that of **2** is given in the Supporting Information (Figure S1). Selected bond lengths and angles are given in Table 1. The bond lengths and angles are similar and, consequently, only those of **2**·C_7H_8 are discussed.

The overall structure of compound **2**·C_7H_8 resembles that of $[Sn(OCH_2CH_2)_2NMe]_2$.[6a] Two stannabicyclooctane units form a *cis*-configured centrosymmetric dimer through intermolecular O→Sn coordination to give a four-membered Sn_2O_2 ring with Sn(1)–O(11) and Sn(1)–O(11A) distances of 2.116(2) and 2.261(2) Å, respectively. Notably, O(11) attached to dimethyl-substituted C(12) is involved in

---

[a] Lehrstuhl für Anorganische Chemie II der Technischen Universität,
44221 Dortmund, Germany
[b] Institut für Organische Chemie, Gutenberg-Universität Mainz,
55099 Mainz, Germany

Supporting information for this article is available on the WWW under http://dx.doi.org/10.1002/ejic.201100352.

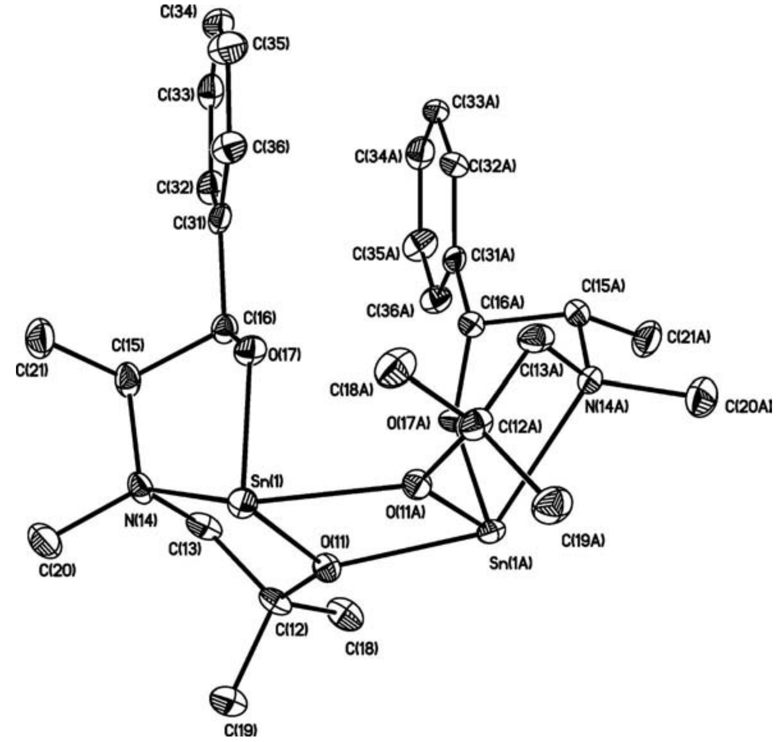

Figure 1. ORTEP presentation of the 30% probability ellipsoids of the depicted atoms and atom numbering scheme of $2\cdot C_7H_8$. The hydrogen atoms are omitted for clarity. The toluene solvate molecule was removed by Squeeze.

the dimerization and not O(17), which is bound to the phenyl-substituted C(16) atom. Also noteworthy are the O(17)···H(16A) and O(17)···H(36) distances of 2.646(4) and 2.389(3) Å, respectively, which might be an indication of weak electrostatic attractions that contribute to the stabilization of the *cis* configuration (Supporting Information, Figure S2). The Sn(1)–N(14) [2.526(3) Å] distance is slightly longer than that in $[Sn(OCH_2CH_2)_2NMe]_2$ [2.447(10) Å].[6a] As a result of the N→Sn coordination, the N(14) atom becomes chiral (*R* configuration).

A ^{119}Sn CP–MAS spectrum of $2\cdot C_7H_8$ shows a single resonance at $\delta_{iso} = -250$ and confirms the presence of only one crystallographic independent tin atom in the solid state. The chemical shift is close to that of the broad resonance at $\delta = -243$ observed in solution, which indicates that **2** is kinetically labile in solution. This is supported by the ESI MS, which revealed a mass cluster centred at *m*/*z* 356 assigned to $[M - H]^+$, but no two tin atom-containing mass cluster. Also present is a mass cluster at *m*/*z* 591, which is assigned to the protonated *spiro*-type compound [**3**-H]$^+$.

The ^{1}H NMR spectrum (500 MHz) of a solution of **2** in CD_2Cl_2 showed, as expected, a doublet resonance for the $NCHCH_3$ protons, two singlet resonances for the nonequivalent $OC(CH_3)$ protons, a singlet for the NCH_3 protons, a doublet of quartet resonance for the NC*H* proton, an AB-type resonance for the NCH_2 protons, a slightly broadened singlet for the OC(Ph)*H* proton and a complex pattern for the phenyl protons.

As a by-product from the reaction shown in Scheme 1, the *spiro*-type compound **3** was formed in a small amount (δ^{119}Sn –448). It was also synthesized by a rational procedure as described below.

The reaction of $Sn(O\text{-}tBu)_4$ with two molar equivalents of the ethanolamine derivative **1** provided the *spiro*-type compound **3** as colourless crystalline material, which is soluble in common organic solvents such as CH_2Cl_2 and toluene (Scheme 2).

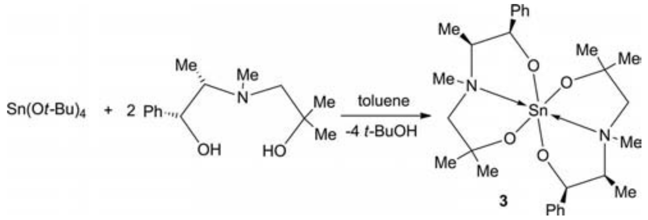

Scheme 2. Synthesis of **3**.

Recrystallization of compound **3** from thf gave single crystals of modification **3a**, and recrystallization from toluene gave single crystals of modification **3b** that were both suitable for X-ray diffraction analysis. Both **3a** and **3b** crystallize in the orthorhombic space group $P2_12_12_1$ but with different cell parameters. The unit cell of **3a** contains four molecules, whereas that of **3b** contains four pairs of crystallographically nonequivalent molecules. The molecular structure of **3a** is shown in Figure 2 and that of **3b** is given in the Supporting Information (Figure S3). Selected bond lengths and angles of **3a** and **3b** are given in Table 1.

Table 1. Selected interatomic distances [Å] and bond angles (°) for **2**·C_7H_8, **2**, **3a** and **3b**.

Interatomic distances				
	2·C_7H_8	**2**	**3a**	**3b**
		($w = 21$, $x = 27$, $y = 11$, $z = 24$)		($w = 31$, $x = 37$, $y = 41$, $z = 34$)
Sn(1)–O(11)	2.116(2)	2.127(2)	1.995(2)	1.981(4)
Sn(1)–O(17)	2.043(2)	2.051(2)	1.999(2)	2.000(4)
Sn(1)–O(11A)	2.261(2)			
Sn(1)–O(21)		2.237(2)	1.988(2)	1.988(4)
Sn(1)–O(27)			2.001(2)	2.005(4)
Sn(1)–N(14)	2.526(3)	2.523(2)	2.438(3)	2.447(5)
Sn(1)–N(24)			2.507(3)	2.497(5)
Sn(2)–O(*w*)		2.136(2)		1.986(4)
Sn(2)–O(*x*)		2.046(2)		1.986(4)
Sn(2)–O(*y*)		2.275(2)		2.009(4)
Sn(2)–O(47)				1.989(4)
Sn(2)–N(*z*)		2.531(3)		2.536(5)
Sn(2)–N(44)				2.414(5)
Bond angles				
O(11)–Sn(1)–O(17)	101.48(9)	101.7(1)	109.6(1)	107.5(2)
O(11)–Sn(1)–O(27)			103.5(1)	105.7(2)
O(11)–Sn(1)–O(11A)	69.60(9)			
O(11)–Sn(1)–N(14)	73.58(8)	72.6(1)	77.4(1)	77.0(2)
O(11)–Sn(1)–N(24)			160.8(1)	159.2(2)
O(11)–Sn(1)–O(21)		69.8(1)	86.5(1)	83.9(2)
O(17)–Sn(1)–O(11A)	84.16(8)			
O(17)–Sn(1)–O(21)		85.5(1)	102.9(1)	105.6(2)
O(17)–Sn(1)–O(27)			135.6(1)	135.0(2)
O(17)–Sn(1)–N(14)	75.68(9)	75.8(1)	76.8(1)	76.2(2)
O(17)–Sn(1)–N(24)			82.1(1)	83.6(2)
O(21)–Sn(1)–O(27)			107.8(1)	107.5(2)
O(21)–Sn(1)–N(24)			75.8(1)	76.1(2)
O(27)–Sn(1)–N(24)			75.4(1)	75.6(2)
N(14)–Sn(1)–O(11A)	133.11(8)			
N(14)–Sn(1)–O(21)		133.2(1)	162.6(1)	160.3(2)
N(14)–Sn(1)–O(27)			82.8(1)	82.6(2)
O(*y*)–Sn(2)–O(*w*)		68.9(1)		87.2(2)
O(*y*)–Sn(2)–O(*x*)		85.9(1)		102.2(2)
O(*y*)–Sn(2)–N(*z*)		133.1(1)		161.0(2)
O(*w*)–Sn(2)–N(*z*)		72.6(1)		75.5(2)
O(*x*)–Sn(2)–N(*z*)		75.4(1)		75.5(2)
O(*w*)–Sn(2)–O(47)				101.7(2)
O(*x*)–Sn(2)–O(47)				139.6(2)
O(*w*)–Sn(2)–O(*x*)				105.1(2)
O(*x*)–Sn(2)–O(*y*)				102.2(2)
O(*y*)–Sn(2)–O(47)				108.8(2)
O(*w*)–Sn(2)–N(44)				162.5(2)
O(*x*)–Sn(2)–N(44)				85.7(2)
O(*y*)–Sn(2)–N(44)				77.0(2)
O(47)–Sn(2)–N(44)				76.9(2)
O(47)–Sn(2)–N(*z*)				82.7(2)
Sn(1)–O(11)–Sn(1A)	109.84(9)			
Sn(1)–O(11)–Sn(2)		109.9(1)		
Sn(1)–O(21)–Sn(2)		111.0(1)		
N(14)–Sn(1)–N(24)			121.0(1)	123.4(2)
N(*z*)–Sn(1)–N(44)				121.1(2)

The Sn(1) atom in **3a** and the Sn(1) and Sn(2) atoms in **3b** each show a distorted octahedral configuration similar to that of Sn[$(OCH_2CH_2)_2NMe$]$_2$[6b] with the N(14) and N(24), and N(34) and N(44) atoms occupying *cis*-positions. The distortion from ideal octahedral geometry is manifested by the O(11)–Sn(1)–N(24), O(21)–Sn(1)–N(14), O(17)–Sn(1)–O(27), O(41)–Sn(2)–N(34), O(31)–Sn(2)–N(44) and O(37)–Sn(2)–O(47) angles of 160.8(1) (**3a**)/159.2(2) (**3b**), 162.6(9) (**3a**)/

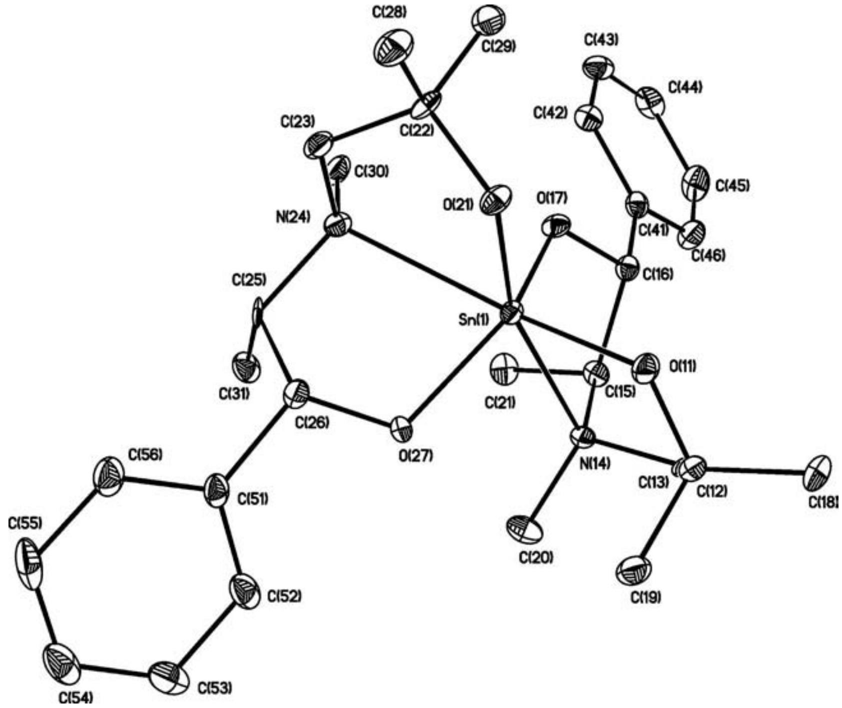

Figure 2. ORTEP presentation of the 30% probability ellipsoids of the depicted atoms and atom numbering scheme of **3a**. The hydrogen atoms are omitted for clarity.

160.3(2) (**3b**), 135.6(1) (**3a**)/135.0(2) (**3b**), 161.0(2), 162.5(2) and 139.6(2)°, respectively, that deviate from the ideal angles of 180°. The intramolecular Sn–N distances vary between 2.414(5) [Sn(2)–N(44)] and 2.536(5) Å [Sn(2)–N(34)], which are longer than the corresponding distances of 2.285(3) and 2.381(3) Å in Sn[(OCH$_2$CH$_2$)$_2$NMe]$_2$.[6b]

The ^{119}Sn NMR spectrum of **3** shows a single resonance at δ = –449, which is identical to that measured for

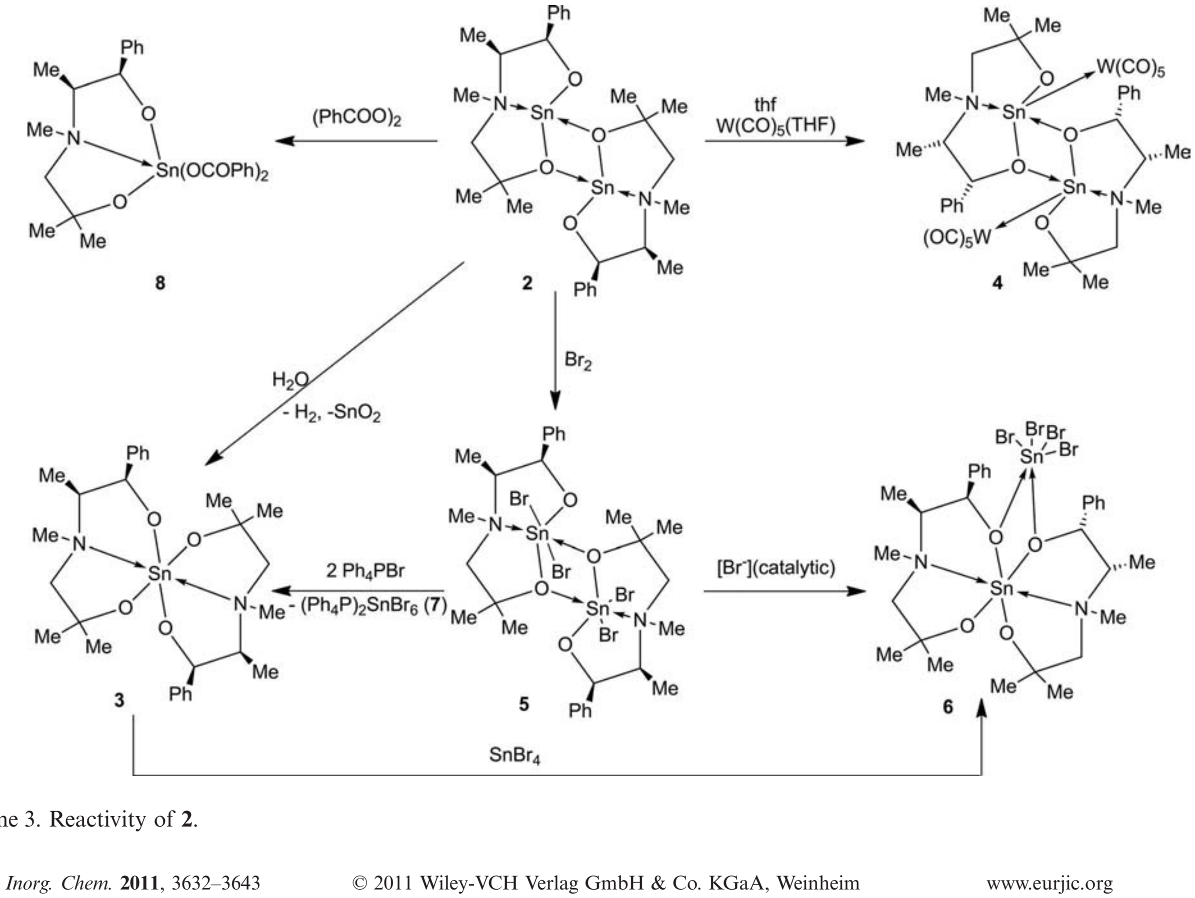

Scheme 3. Reactivity of **2**.

$Sn[(OCH_2CH_2)_2NMe]_2$.[6b] Notably, the ^{119}Sn CP–MAS spectrum of **3b** revealed two signals at δ_{iso} = –450.5 and –452.2, which are consistent with the two crystallographically nonequivalent tin atoms and are close to the chemical shift observed in solution indicating similar structures in both states. This contrasts with the observation made for $Sn[(OCH_2CH_2)_2NMe]_2$,[6b] which showed different ^{119}Sn chemical shifts in solution and in the solid state.

The ^1H NMR spectrum of **3** in C_6D_6 solution showed the expected resonances, as discussed above for **2** (Scheme 3).

The stannylene **2** reacts in thf with in situ prepared $W(CO)_5{\cdot}THF$ to give the corresponding tungsten pentacarbonyl complex **4**, which was isolated as the colourless crystalline toluene solvate **4**$\cdot C_7H_8$ after recrystallization from toluene.

The molecular structure of **4**$\cdot C_7H_8$ is shown in Figure 3, and selected bond lengths and angles are given in Table 2. The stannylene transition metal complex **4**$\cdot C_7H_8$ crystallized in the monoclinc space group *P*2 with four crystallographically independent tin atoms in the unit cell.

The overall structure of **4**$\cdot C_7H_8$ resembles that of $[MeN(CH_2CH_2O)_2SnW(CO)_5]_2$.[6a] Four stannabicyclooctane complexes form two *cis*-configured dimers through intermolecular O→Sn coordination to give four-membered Sn_2O_2 rings with Sn(1)–O(27)/Sn(2)–O(17) and Sn(3)–O(47)/Sn(4)–O(37) distances of 2.205(4)/2.190(4) and 2.203(4)/2.203(4) Å, respectively. Notably, in contrast to **2**$\cdot C_7H_8$, O(17)/O(27) and O(37)/O(47) attached to the phenyl-substituted C(16)/C(26) and C(36)/C(46) atoms, respectively, are involved in the dimerization and not O(11)/O(21) and O(31)/O(41), which are bound to dimethyl-substituted C(12)/C(22) and C(36)/C(46) atoms, respectively. The intramolecular Sn–N distances fall in a narrow range between 2.336(5) [Sn(3)–N(34), Sn(4)–N(44)] and 2.348(5) Å [Sn(2)–N(24)] and are shorter than those in **2**$\cdot C_7H_8$ but similar to those in $[MeN(CH_2CH_2O)_2SnW(CO)_5]_2$ [2.356(5), 2.360(6) Å].[6a] The Sn–W distances, between 2.731(5) [Sn(1)–W(1)] and 2.743(5) Å [Sn(4)–W(4)], are close to those of $[MeN(CH_2CH_2O)_2SnW(CO)_5]_2$ [2.7275(12), 2.7369(10) Å].[6a]

The ^{119}Sn CP–MAS spectrum revealed three signals at δ_{iso} = –166.0 (integral: ca. 2), –171.5 (integral: ca. 1) and –177.8 (integral: ca. 1), which reflect the four crystallographically independent tin atoms, with two signals being superimposed.

The ^{119}Sn NMR spectrum in CD_2Cl_2 of compound **4** showed two resonances at δ = –169.6 [$^1J(^{119}Sn–^{183}W)$ 1493 Hz, integral 1] and δ = –198.4 [$^1J(^{119}Sn–^{183}W)$ 1576 Hz, $^2J(^{117}Sn–O–^{119}Sn)$ 157 Hz, integral 3]. As result of poor solubility, no $^2J(^{117}Sn–O–^{119}Sn)$ satellites were observed for the low intensity signal. The ^1H and ^{13}C NMR spectra of the same solution displayed two sets of signals with the integration ratio of 1:3.

The results are interpreted with caution in terms of an equilibrium between the two dimers **4** and **4a**, which is slow on the NMR time scale but fast on the laboratory time scale (Scheme 4). A monomer–dimer equilibrium is less likely as the difference between the two ^{119}Sn chemical shifts is not big enough to account for tin atoms with dif-

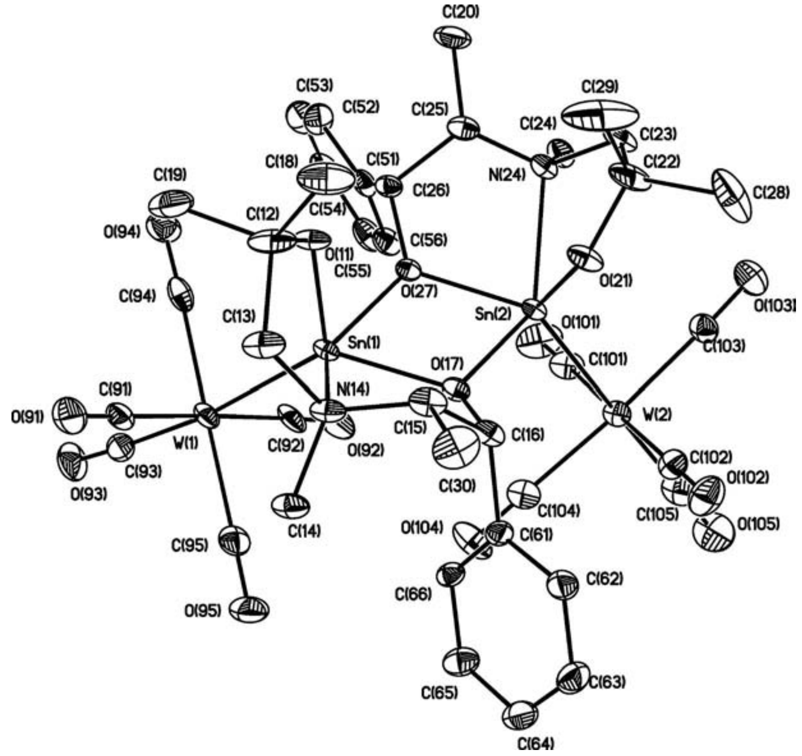

Figure 3. ORTEP presentation of the 30% probability ellipsoids of the depicted atoms and atom numbering scheme of **4**$\cdot C_7H_8$. The hydrogen atoms and the disordered toluene molecules are omitted for clarity.

Table 2. Selected interatomic distances [Å] and bond angles (°) for $4 \cdot C_7H_8$.

Interatomic distances		Bond angles	
Sn(1)–O(11)	2.002(4)	O(11)–Sn(1)–O(17)	105.6(2)
Sn(1)–O(17)	2.086(4)	O(11)–Sn(1)–O(27)	84.6(2)
Sn(1)–O(27)	2.205(4)	O(11)–Sn(1)–N(14)	77.6(2)
Sn(1)–N(14)	2.340(5)	O(17)–Sn(1)–O(27)	70.8(2)
		O(17)–Sn(1)–N(14)	76.9(2)
		O(27)–Sn(1)–N(14)	137.0(2)
Sn(2)–O(21)	1.999(4)	O(21)–Sn(2)–O(27)	106.6(2)
Sn(2)–O(27)	2.097(4)	O(21)–Sn(2)–O(17)	84.3(2)
Sn(2)–O(17)	2.190(4)	O(21)–Sn(2)–N(24)	77.5(2)
Sn(2)–N(24)	2.348(5)	O(27)–Sn(2)–O(17)	70.9(2)
		O(27)–Sn(2)–N(24)	76.2(2)
		O(17)–Sn(2)–N(24)	135.7(2)
Sn(3)–O(31)	2.005(4)	O(31)–Sn(3)–O(37)	104.4(2)
Sn(3)–O(37)	2.097(4)	O(31)–Sn(3)–O(47)	85.6(2)
Sn(3)–O(47)	2.203(4)	O(31)–Sn(3)–N(34)	77.5(2)
Sn(3)–N(34)	2.336(5)	O(37)–Sn(3)–O(47)	70.7(1)
		O(37)–Sn(3)–N(34)	76.7(2)
		O(47)–Sn(3)–N(34)	138.1(2)
Sn(4)–O(41)	1.990(5)	O(41)–Sn(4)–O(47)	107.0(2)
Sn(4)–O(47)	2.107(4)	O(41)–Sn(4)–O(37)	84.9(2)
Sn(4)–O(37)	2.203(4)	O(41)–Sn(4)–N(44)	78.7(2)
Sn(4)–N(44)	2.336(5)	O(47)–Sn(4)–O(37)	70.6(1)
		O(47)–Sn(4)–N(44)	76.3(2)
		O(37)–Sn(4)–N(44)	136.6(2)
Sn(1)–W(1)	2.731(5)	W(1)–Sn(1)–O(11)	125.1(2)
Sn(2)–W(2)	2.740(5)	W(1)–Sn(1)–O(17)	129.1(1)
Sn(3)–W(3)	2.736(5)	W(1)–Sn(1)–O(27)	107.3(1)
Sn(4)–W(4)	2.743(5)	W(1)–Sn(1)–N(14)	115.1(1)
		W(2)–Sn(2)–O(21)	123.8(2)
		W(2)–Sn(2)–O(27)	129.5(1)
		W(2)–Sn(2)–O(17)	107.7(1)
		W(2)–Sn(2)–N(24)	116.0(1)
		W(3)–Sn(3)–O(31)	124.1(1)
		W(3)–Sn(3)–O(37)	131.4(1)
		W(3)–Sn(3)–O(47)	106.8(1)
		W(3)–Sn(3)–N(34)	114.6(1)
		W(4)–Sn(4)–O(41)	123.3(2)
		W(4)–Sn(4)–O(47)	129.3(1)
		W(4)–Sn(4)–O(37)	106.3(1)
		W(4)–Sn(4)–O(44)	116.3(1)
Sn(1)···Sn(2)	3.496(6)	Sn(1)–O(17)–Sn(2)	109.7(2)
O(17)···O(27)	2.486(6)	Sn(1)–O(27)–Sn(2)	108.7(2)
Sn(3)···Sn(4)	3.509(6)	Sn(3)–O(37)–Sn(4)	109.3(2)
O(37)···O(47)	2.491(5)	Sn(3)–O(47)–Sn(4)	109.0(2)

ferent coordination numbers. The alternative dimer **4b**, in which two chemically nonequivalent oxygen atoms form the bridge, can be excluded as the ^{1}H NMR spectrum should reveal three sets of signals if this were present.

The positive mode ESI MS of compound **4** showed a high-intensity mass cluster centred at *m*/*z* 1378.2 that is assigned to the cation $[4 \cdot Na]^+$. There was also a mass cluster of lower intensity (≈ 40 %) centred at *m*/*z* 743.2, which is assigned to $[C_{14}H_{21}NO_2SnW(CO)_4(C_7H_8)]^+$.

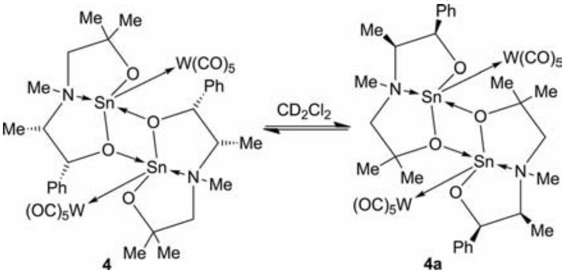

Scheme 4. Equilibrium between **4** and **4a**.

The reaction of the stanna(II)bicyclooctane **2** with Br_2 gave a crude reaction mixture from which the Sn^{IV} compound **5** was isolated as colourless crystalline material. After the mother liquor had been stored for several days in sunlight, slightly red crystals of the rearrangement product **6**, as its toluene solvate $6 \cdot C_7H_8$, separated. Both **5** and $6 \cdot C_7H_8$ are poorly soluble in organic solvents such as CH_2Cl_2, thf and dmso. The formation of $6 \cdot C_7H_8$ from **5** might be catalyzed by traces of bromide in the reaction mixture. This hypothesis is supported by the reaction of **5** with two molar equivalents of Ph_4PBr that provides compound **3** and bis(tetraphenylphosphonium)hexabromidostannate (**7**). Compound $6 \cdot C_7H_8$ was also obtained from the reaction of **3** with $SnBr_4$ (Scheme 3).

The molecular structure of **5** is shown in Figure 4, and selected bond lengths and angles are given in Table 3. Compound **5** crystallizes in the monoclinic space group $P2_1$ with two molecules in the unit cell. The two stanna(IV)bicyclooctane units form a *trans*-configured dimer through intermolecular O→Sn coordination to give a four-membered Sn_2O_2 ring with Sn(1)–O(11)/Sn(1)–O(21) and Sn(2)–O(11)/Sn(2)–O(21) distances of 2.172(6)/2.091(5) and 2.075(5)/2.150(6) Å, respectively. As in **2** and $2 \cdot C_7H_8$, at first sight the dimerization takes place through the O(11)/O(21) atoms that are bound to the dimethyl-substituted carbon atoms C(12)/C(22). However, a close inspection of the structure revealed that the Sn(1)–O(11) [2.172(6) Å] and Sn(2)–O(21) [2.150(6) Å] distances are considerably longer than the Sn(1)–O(21) [2.091(5) Å] and Sn(2)–O(11) [2.075(5) Å] distances. With caution, this observation might be interpreted in terms of a snapshot of a ring opening dimerization of **5** from two bis(μ-oxido)-bridged eight-membered stannabicyclooctanes to a sixteen-membered ring. Both the Sn(1) and Sn(2) atoms are hexacoordinate and show a distorted octahedral configuration with the Br(1)/Br(2) (at Sn1) and Br(3)/Br(4) atoms (at Sn2) being *cis* to each other. The distortion from ideal octahedral geometry is manifested by the deviation of the N(14)–Sn(1)–O(21) [147.8(2)°] and N(24)–Sn(2)–O(11) [152.6(3)°] angles from 180°. The other *trans* angles fall in the range between 172.9(1) [Br(2)–Sn(1)–O(17)] and 179.2(2)° [Br(3)–Sn(2)–O(21)]. The Sn(1)–N(14) [2.283(6) Å] and Sn(2)–N(24) [2.226(6) Å] distances differ slightly and are the shortest of the compounds reported in this paper. The Sn–Br distances fall in the narrow range from 2.533(2) [Sn(1)–Br(2)] to 2.548(2) Å [Sn(2)–Br(3)], which is slightly shorter than the

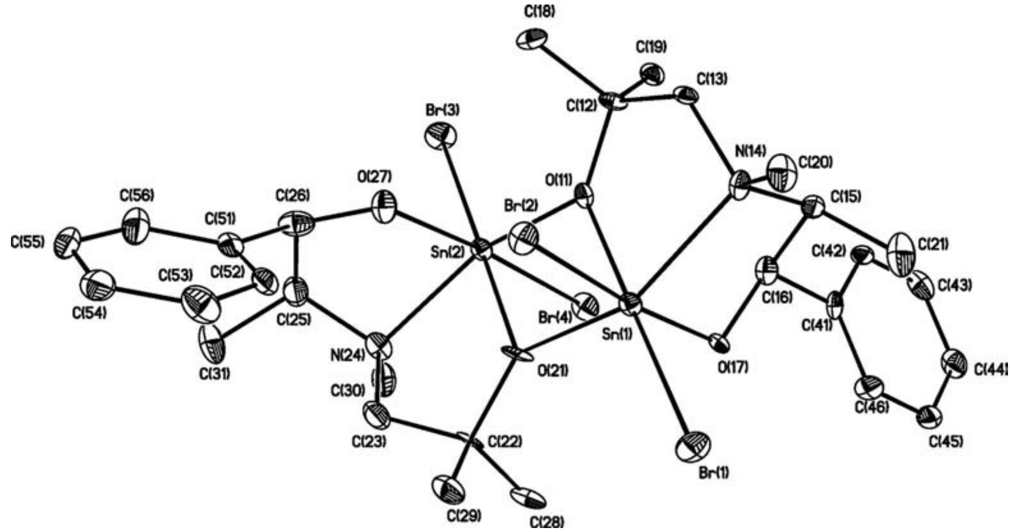

Figure 4. ORTEP presentation of the 30% probability ellipsoids of the depicted atoms and atom numbering scheme of **5**. The hydrogen atoms are omitted for clarity.

corresponding distances in **7** [2.562(4)–2.624(5) Å] and bis(2,6-diamino-3,5-dibromopyridinium) hexabromidostannate [2.577(1)–2.613(1) Å].[7]

The ^{119}Sn CP–MAS NMR spectrum of compound **5** showed a single resonance at $\delta_{\text{iso}} = -503$, which does not distinguish between the two crystallographically independent Sn(1) and Sn(2) atoms found by single-crystal X-ray diffraction analysis.

The molecular structure of **6**·C_7H_8 is shown in Figure 5, and selected bond lengths and angles are given in Table 3. Compound **6**·C_7H_8 is composed of the Lewis acid tin tetrabromide and the Lewis base **3** that coordinates through the O(17)/O(17A) oxygen atoms at a distance of 2.153(6) Å. As a result, the Sn(2) atom becomes hexacoordinate with a distorted octahedral configuration manifested by the Br(1)–Sn(1)–O(17A) and Br(2)–Sn(1)–Br(2A) angles of 165.4(1) and 172.3(1)°, respectively. The Sn(1)–Br(1) and Sn(2)–Br(2) distances of 2.530(1) and 2.568(1) Å, respectively, are close to those in compound **5** (see above). The Sn(1) atom is also six-coordinate bound to O(11), O(11A), O(17), O(17A), N(14) and N(14A). Its configuration can be interpreted as being derived from a square pyramid in which the apical position is split into two sides that are occupied by the O(17)/O(17A) atoms at a Sn(1)–O(17) distance of 2.093(6) Å and a O(17)···O(17A) separation of 2.482(8) Å. Alternatively, the configuration can also be seen as being derived from a distorted SnO_4 terahedron that is doubly face-attacked by N(14) and N(14A) with a Sn(1)–N(14) distance of 2.340(8) Å. To some extent the structure of **6**·C_7H_8 resembles that of the complex formed between Ph_2SnCl_2 and the ethanolamine derivative $Ph_2Sn(OCH_2CH_2NMe_2)_2$ in which the latter coordinates the former through two oxygen atoms with a Sn(1)–O(1)/O(1A) distance of 2.242(3) Å.[1g]

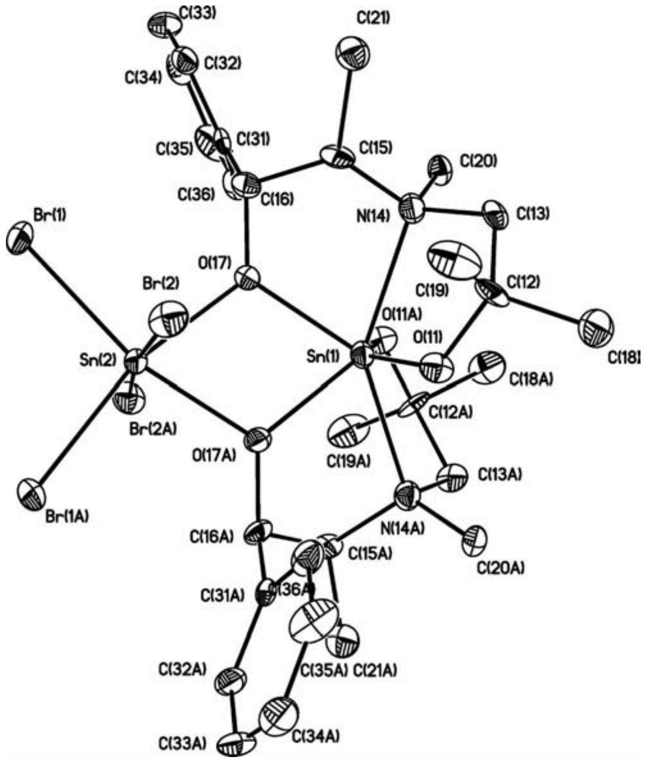

Figure 5. ORTEP presentation of the 30% probability ellipsoids of the depicted atoms and atom numbering scheme of **6**·C_7H_8. The hydrogen atoms and the disordered toluene molecule are omitted for clarity.

The ^{119}Sn CP–MAS NMR spectrum of **6**·C_7H_8 shows a resonance at $\delta_{\text{iso}} = -506$ belonging to Sn(1) and a broad hump-like resonance at $\delta_{\text{iso}} = -1404$ assigned to Sn(2), which is similar to the that observed for *trans*-$SnBr_4$·$2Bu_3P(O)$ ($\delta = -1479$) and *cis*-$SnBr_4$·acetone ($\delta = -1383$).[7]

Compound **7** is only the second example of a hexabromidostannate salt.[8] Its molecular structure is shown in Figure 6, and selected bond lengths and angles are given in the figure caption. The stannate anion shows slightly distorted

Table 3. Selected interatomic distances [Å] and bond angles (°) for **5** and **6**·C_7H_8.

Interatomic distances			
	5	**6**·C_7H_8	
Sn(1)–O(11)	2.172(6)	1.949(6)	
Sn(1)–O(17)	1.984(6)	2.093(6)	
Sn(1)–O(21)	2.091(5)		
Sn(1)–N(14)	2.283(6)	2.340(8)	
Sn(2)–O(21)	2.150(6)		
Sn(2)–O(27)	2.003(6)		
Sn(2)–O(11)	2.075(5)		
Sn(2)–O(17)		2.153(6)	
Sn(2)–N(24)	2.226(6)		
Sn(1)–Br(1)	2.537(2)		
Sn(1)–Br(2)	2.533(2)		
Sn(2)–Br(3)	2.548(2)		
Sn(2)–Br(4)	2.544(2)		
Sn(2)–Br(1)		2.529(1)	
Sn(2)–Br(2)		2.568(1)	
Sn(1)···Sn(2)	3.405(8)	3.446(6)	
O(11)···O(21)	2.534(9)		
O(17)···O(17A)		2.482(8)	
Bond angles			
O(11)–Sn(1)–O(17)	90.5(2)		117.7(3)
O(11)–Sn(1)–O(21)	72.87(19)	O(11)–Sn(1)–O(11A)	137.9(4)
O(11)–Sn(1)–N(14)	75.2 (2)		79.7(3)
O(17)–Sn(1)–O(21)	94.2 (2)	O(11)–Sn(1)–O(17A)	96.5(2)
O(17)–Sn(1)–N(14)	81.4 (2)		74.6(3)
O(21)–Sn(1)–N(14)	147.8(2)	O(11)–Sn(1)–N(14A)	87.3(3)
		O(17)–Sn(1)–O(17A)	72.7(3)
O(11)–Sn(2)–O(21)	73.6(2)	O(17)–Sn(1)–N(14A)	140.5(3)
O(11)–Sn(2)–O(27)	92.7(2)	N(14)–Sn(1)–N(14A)	143.4(4)
O(11)–Sn(2)–N(24)	152.6(3)	O(17)–Sn(2)–O(17A)	70.4(3)
O(21)–Sn(2)–O(27)	89.1(3)		
O(21)–Sn(2)–N(24)	80.0(3)		
O(27)–Sn(2)–N(24)	79.6(3)		
Br(1)–Sn(1)–O(11)	177.39(15)		
Br(1)–Sn(1)–O(17)	87.08(9)	Br(1)–Sn(2)–O(17)	95.02(15)
Br(1)–Sn(1)–O(21)	106.32(15)	Br(1)–Sn(2)–O(17A)	165.41(15)
Br(1)–Sn(1)–N(14)	105.3(2)		
Br(2)–Sn(1)–O(11)	90.78(15)		
Br(2)–Sn(1)–O(17)	172.94(13)	Br(2)–Sn(2)–O(17)	87.66(16)
Br(2)–Sn(1)–O(21)	92.77(17)	Br(2)–Sn(2)–O(17A)	86.04(16)
Br(2)–Sn(1)–N(14)	92.22(18)		
Br(3)–Sn(2)–O(11)	106.65(16)		
Br(3)–Sn(2)–O(21)	179.22(17)		
Br(3)–Sn(2)–O(27)	90.1(2)		
Br(3)–Sn(2)–N(24)	99.7(2)		
Br(4)–Sn(2)–O(11)	92.18(16)		
Br(4)–Sn(2)–O(21)	91.26(17)		
Br(4)–Sn(2)–O(27)	174.99(15)		
Br(4)–Sn(2)–N(24)	95.6 (2)	Br(1)–Sn(2)–Br(1A)	99.57(6)
		Br(2)–Sn(2)–Br(2A)	172.28(7)
Br(1)–Sn(1)–Br(2)	91.75(4)	Br(1)–Sn(2)–Br(2)	93.50(4)
Br(3)–Sn(2)–Br(4)	89.46(4)	Br(2)–Sn(2)–Br(1A)	91.48(4)

octahedral configuration with all *trans*-Br–Sn–Br angles equal to 180°, and the Sn–Br distances lie between 2.5620(4) [Sn(1)–Br(2)] and 2.6242(5) Å [Sn(1)–Br(3)]. The different bond lengths are the result of weak Br(1)···H(45A), Br(2)···H(32A) and Br(3)···H(44A) electrostatic interactions at distances of 3.010(1), 2.87(1) and 3.180(1) Å, respectively.

The stannylene **2** reacts with $[PhC(O)O]_2$ under oxidative addition to give **8** as a white amorphous, sharp melting material. Compound **8** is soluble in common organic solvents such as toluene, THF and CH_2Cl_2. The ^{119}Sn NMR spectrum in C_6D_6 shows a singlet resonance at δ –565. The ^{1}H and ^{13}C NMR spectra are as expected and show no peculiarities. Single crystals suitable for X-ray diffraction analysis were not obtained.

Conclusions

A variety of tin(II) and tin(IV) derivatives of the enantiopure ephedrine-based ethanolamine $MeN(CH_2CMe_2OH)$-[(*S*)-CH(Me)-(*R*)-CH(Ph)OH] is reported. A characteristic feature for the stannylene **2**, its tungstenpentacarbonyl complex **4**·C_7H_8 and the bromido-substituted tin(IV) derivative **5** is dimerization through intermolecular O→Sn interactions. In the case of compound **2** (both for solvent-free **2** and the toluene solvate **2**·C_7H_8) the dimer adopts a *cis* configuration that appears to be supported by a number of C–H···O electrostatic interactions. Of particular interest is the bromide anion-catalyzed rearrangement of **5** to give the unprecedented tin tetrabromide complexed *spiro*-type compound **6**·C_7H_8. Preliminary studies on the ability of compounds **3** and **8** to catalyze the ring-opening polymerization of DL-lactide were promising as both compounds gave yields above 90 % and polymers of high molecular mass (see Supporting Information, Table S1).

Experimental Section

General Methods: All solvents were purified by distillation under argon from appropriate drying agents. All reactions were carried out under an inert atmosphere of argon. The NMR experiments were carried out with Bruker DRX 400 and Bruker DPX 300 spectrometers. Chemical shifts are given in ppm and are referenced to the solvent peaks with the usual values calibrated against tetramethylsilane (^{1}H, ^{13}C) and tetramethylstannane (^{119}Sn). The electrospray mass spectra were recorded with a Thermoquest-Finnigan instrument using CH_3CN or CH_2Cl_2 as the mobile phase. The samples were introduced as solution with a syringe pump operating at a rate of 0.5 μL min^{-1}. The capillary voltage was 4.5 kV and the cone skimmer voltage varied between 50 and 250 kV. Identification of the expected ions was assisted by comparison of experimental and calculated isotope distribution patterns. Elemental analyses were performed with a LECO-CHNS-932 analyser.

Crystallography: Intensity data for colourless crystals of **2**, **2**·C_7H_8, **3a**, **3b**, **5**, **6**·C_7H_8 and **7** were collected with an Xcalibur2 CCD diffractometer (Oxford Diffraction) and those for **4**·C_7H_8 with a SMART CCD diffractometer (Bruker) with graphite-monochromated Mo-K_α radiation at 110 K (**2**·C_7H_8, **2**, **3a**, **4**·C_7H_8, **5**, **6**·C_7H_8 and **7**) and 295 K (**3b**). The data collection covered almost the whole sphere of the reciprocal space with 9 (**2**·C_7H_8), 8 (**2**), 6 (**3a**), 5 (**3b**), 31 (**4**·C_7H_8), 4 (**5**), 2 (**6**·C_7H_8) and 7 (**7**) sets at different κ-angles and 401 (**2**·C_7H_8), 449 (**2**), 278 (**3a**), 227 (**3b**), 1952 (**4**·C_7H_8),

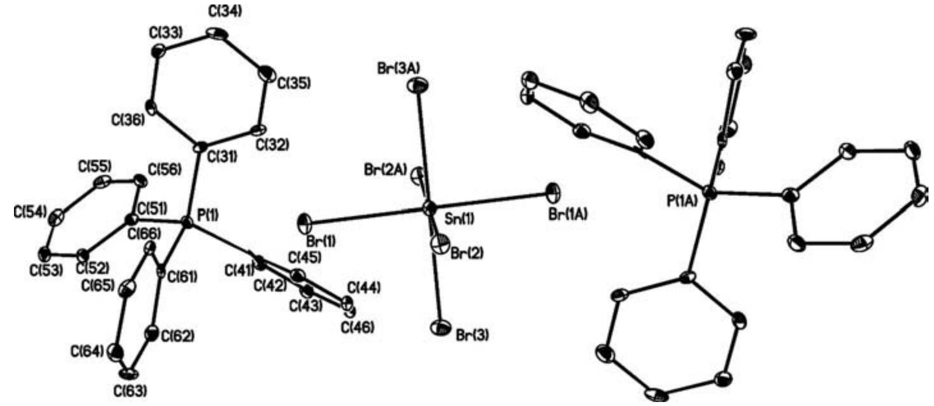

Figure 6. ORTEP presentation of the 30% probability ellipsoids of the depicted atoms and atom numbering scheme of **7** {$P\bar{1}$ [Z = 1, a = 10.3644(7), b = 10.5036(7), c = 12.1289(8), α = 92.636(6), β = 99.939(6), γ = 117.168(7); V = 1145.29(13), R_{int} = 0.00392, R_1 = 0.0298, wR_2(all data) = 0.0467; GooF = 0.817, Completenes to 25.50 θ = 99.7%]}. The hydrogen atoms were omitted for clarity. Bond lengths: Sn(1)–Br(1) 2.6120(5), Sn(1)–Br(2) 2.5620(4), Sn(1)–Br(3) 2.6242(5) Å; bond angles: Br(1)–Sn(1)–Br(1A) = Br(2)–Sn(1)–Br(2A) = Br(3)–Sn(1)–Br(3A) = 180.00(2)°.

284 (**5**), 117 (**6**·C_7H_8) and 445 (**7**) frames via ω-rotation (Δ/ω = 1°) at two times 8 (**2**·C_7H_8), 1.5 (**2**), 15 (**3a**), 50 (**3b**), 10 (**4**·C_7H_8), 2.7 (**5**), 10 (**6**·C_7H_8) and 3 s (**7**) per frame. The crystal-to-detector distance was 4.5 cm. Crystal decay was monitored by repeating the initial frames at the end of data collection. Analysis of the duplicate reflection indicated that there was no decay. The structures were solved by direct methods SHELXS97[9] and successive difference Fourier syntheses. Refinement applied full-matrix least-squares methods SHELXL97.[10] All H atoms were located in the difference Fourier map and their positions were isotropically refined with U_{iso} constrained at 1.2 times U_{eq} of the carrier C atom for nonmethyl and 1.5 times U_{eq} of the carrier C atom for methyl groups. Atomic scattering factors for neutral atoms and real and imaginary dispersion terms were taken from the *International Tables for X-ray Crystallography*.[11] The toluene molecule in **2**·C_7H_8 was found to be severely disordered and could not be modelled effectively. To improve the refinement for the main structure the solvent molecule was removed by Squeeze (Platon).[12] In order to refine the disorder of the solvate molecules in **4** and **6** satisfactorily, ISOR restraints were used. The figures were created with SHELXTL.[13] Crystallographic data are given in Table 4 and in the Supporting Information (Figure S3).

CCDC-819609 (for **2**·C_7H_8), -819606 (for **2**), -819605 (for **3a**), -819607 (for **3b**), -819602 (for **4**·C_7H_8), -819608 (for **5**), -819603 (for **6**·C_7H_8) and -819604 (for **7**) contain the supplementary crystallographic data for this paper. These data can be obtained free of charge from The Cambridge Crystallographic Data Centre via www.ccdc.cam.ac.uk/data_request/cif.

^{119}Sn CP–MAS Spectroscopy: The ^{119}Sn CP–MAS NMR spectra were recorded with a Bruker Avance III 400 spectrometer using cross polarization and high-power proton decoupling [conditions: 3.7 µs (90°) pulse, contact times between 5 and 8 ms, 10 s recycle delay]. Spectra with different spinning rates between 5 and 9 kHz were recorded in order to unambiguously determine the isotropic chemical shifts. Tetracyclohexyltin was used as secondary reference (δ = 97.35 ppm).

[MeN(CH$_2$CMe$_2$O){(*S*)-CH(Me)-(*R*)-CH(Ph)O}Sn]$_2$ (2): A suspension of $Sn(OMe)_2$ (5.41 g, 2.99 mmol) in toluene (250 mL) was heated to reflux and excess *n*-butanol (50 mL) was added. The reaction mixture became a clear solution and the methanol/toluene azeotropic mixture was removed by distillation. The ethanolamine derivative $MeN(CH_2CMe_2OH)$[(*S*)-CH(Me)-(*R*)-CH(Ph)OH][14] (**1**) (7.12 g, 3.00 mmol) was added. After the butanol/toluene mixture and one third of the toluene had been removed by distillation and the reaction mixture had been cooled to room temperature, hexagonal crystals (10.2 g, 85%, m.p. 217 °C) of **2**, as its toluene solvate **2**·C_7H_8, were obtained, which were suitable for single-crystal X-ray diffraction studies. The crystals were dried in vacuo. ^{1}H and ^{13}C NMR spectroscopy as well as elemental analysis confirmed the presence of a toluene molecule in the unit cell. ^{1}H NMR (400.13 MHz, CD_2Cl_2): δ = 7.31–6.98 (m, 15 H, H_{arom} + $H_{toluene}$), 5.42 [d, $^3J(^1H–^1H)$ = 2 Hz, 2 H, PhC*H*OSn], 3.04 [d, $^2J(^1H–^1H)$ = 13 Hz, 2 H, NC*H*H], 2.66 [dq, $^3J(^1H–^1H)$ = 2, $^3J(^1H–^1H)$ = 7 Hz, 2 H, NC*H*CH$_3$], 2.54 [s, $^3J(^1H–^{119}Sn)$, 6 H, NC*H*$_3$], 2.52 [d, $^2J(^1H–^1H)$ = 13 Hz, 2 H, NC*H*$_2$], 2.23 [s, 3H, $CH_{3(toluene)}$] 1.50 [s, 6 H, OC(Me)C*H*$_3$], 1.45 [s, 6 H, OC(*Me*)CH$_3$], 0.61 [d, 6 H, $^3J(^1H–^1H)$ = 7 Hz, NCHC*H*$_3$] ppm. $^{13}C\{^1H\}$ NMR (100.63 MHz, CD_2Cl_2): δ 145.9 (C_i), 138.1 ($C_{i(toluene)}$),129.4($C_{o(toluene)}$), 128.6 (C_o), 128.4 ($C_{m(toluene)}$), 127.8 (C_p), 126.8 (C_m), 125.5 ($C_{p(toluene)}$), 75.7 (PhCH), 74.8 (NCH), 72.8 [*C*(CH$_3$)$_2$], 69.8 (NCH$_2$), 42.1 (NCH$_3$), 27.2, 27.0 [C(*C*H$_3$)$_2$], 21.6 (CH$_3$, toluene), 10.6 (NCH*C*H$_3$) ppm. $^{119}Sn\{^1H\}$ NMR (111.9 MHz, CD_2Cl_2): δ = –242 (broad signal $\nu_{1/2}$ = 815 Hz) ppm. $C_{35}H_{50}N_2O_4Sn_2$ (800.20): calcd. C 52.5, H 6.3, N 3.5; found C 52.3, H 6.3, N 3.5.

Recrystallization from donor solvents such as pyridine, *n*Bu$_2$O, HMPA, dioxane or THF gave colourless solvate-free crystals **2** (m.p. 234 °C), suitable for single-crystal X-ray diffraction studies. ^{1}H NMR (500.13 MHz, CD_2Cl_2): δ 7.28–6.99 (m, 10 H, H_{arom}), 5.42 [d, $^3J(^1H–^1H)$ = 2 Hz, 2 H, PhC*H*OSn], 3.04 [d, $^2J(^1H–^1H)$ = 13 Hz, 2 H, NC*H*H], 2.66 [dq, $^3J(^1H–^1H)$ = 2 Hz, $^3J(^1H-^1H)$ = 7 Hz, 2 H, NC*H*CH$_3$], 2.54 [s, $^3J(^1H–^{119}Sn)$, 6 H, NC*H*$_3$], 2.52 [d, $^2J(^1H–^1H)$ = 13 Hz, 2 H, NC*H*$_2$], 1.50 [s, 6 H, OC(Me)C*H*$_3$], 1.45 [s, 6 H, OC(*Me*)CH$_3$], 0.61 [d, 6 H, $^3J(^1H–^1H)$ = 7 Hz, NCHC*H*$_3$] ppm. $^{13}C\{^1H\}$ NMR (100.63 MHz, CD_2Cl_2): δ 145.9 (C_i), 128.6 (C_o), 127.8 (C_p), 126.8 (C_m), 75.7 (PhCH), 74.8 (NCH), 72.8 [*C*(CH$_3$)$_2$], 69.8 (NCH$_2$), 42.1 (NCH$_3$), 27.2, 27.0 [C(*C*H$_3$)$_2$], 10.6 (NCH*C*H$_3$) ppm. $^{119}Sn\{^1H\}$ NMR (111.9 MHz, CD_2Cl_2): δ = –243 (broad signal, $\nu_{1/2}$ = 853 Hz) ppm. ^{119}Sn CP–MAS NMR (149.23 MHz): δ = –250 ppm. $C_{28}H_{42}N_2O_4Sn_2$ (708.06 g/mol): calcd. C 47.5, H 6.0, N 4.0; found C 47.3, H 6.1, N 4.0. LC ESI MS: Calculated for $[C_{14}H_{28}NO_2{}^{120}Sn + H^+]^+$ 356.1, found 356.0.

Table 4. Crystal data and structure refinement for **2**·C_7H_8, **2**, **3a**, **4**·C_7H_8, **5** and **6**·C_7H_8.[a]

	2·C_7H_8	**2**	**3a**
Empirical formula	$C_{28}H_{42}N_2O_4Sn_2$	$C_{28}H_{42}N_2O_4Sn_2$	$C_{28}H_{42}N_2O_4Sn$
Formula weight	708.02	708.02	589.33
Temperature [K]	173(1)	173(1)	173(1)
Wavelength [Å]	0.71073	0.71073	0.71073
Crystal system	hexagonal	monoclinic	orthorhombic
Space group	$P3_12_1$	$P2_1$	$P2_12_12_1$
a [Å]	10.9234(15)	11.7099(3)	10.8701(4)
b [Å]	10.9234(15)	9.6573(2)	14.6522(6)
c [Å]	25.437(5)	13.0878(3)	17.0658(7)
α [°]	90	90	90
β [°]	90	94.424(2)	90
γ [°]	120	90	90
Volume /Å^3	2628.5 (7)	1475.64(6)	2718.1(2)
Z	3	2	4
D_c [g/cm^3]	1.342	1.593	1.440
Abs. coeff. [mm^{-1}]	1.454	1.726	0.975
F(000)	1068	712	1224
Crystal size [mm]	0.40 × 0.22 × 0.08	0.28 × 0.20 × 0.20	0.22 × 0.18 × 0.16
θ range for data collection	2.15–25.50	2.25–25.50	2.22–25.50
Reflections collected	19274	12963	13804
Independent reflections	3269 [R(int) = 0.055]	5283 [R(int) = 0.031]	5042 [R(int) = 0.0390]
Completeness to θ = 25.50°	99.7%	99.9%	99.9%
Refinement method		Full matrix least-squares on F^2	
Data/restraints/parameters	3273/0/167	5283/1/333	5042/0/323
Goodness-of-fit on F^2	0.932	0.922	0.676
Final R indices	R_1 = 0.0221,	R_1 = 0.0218,	R_1 = 0.0267,
[$I > 2\sigma(I)$]	wR_2 = 0.0437	wR_2 = 0.0433	wR_2 = 0.0422
R indices	R_1 = 0.0266,	R_1 = 0.0259,	R_1 = 0.0398,
(all data)	wR_2 = 0.0440	wR_2 = 0.0439	wR_2 = 0.0433
Largest diff. peak and hole [e·Å^{-3}]	0.946 and –0.501	0.262 and –0.440	0.550 and –0.478
	4·C_7H_8	**5**	**6**·C_7H_8
Empirical formula	$C_{38}H_{42}N_2O_{14}Sn_2W_2 \cdot C_7H_8$	$C_{28}H_{42}Br_4N_2O_4Sn_2$	$C_{28}H_{42}Br_4N_2O_4Sn_2 \cdot C_7H_8$
Formula weight	1447.95	1027.66	1119.79
Temperature [K]	173(1)	173(1)	173(1)
Wavelength [Å]	0.71073	0.71073	0.71073
Crystal system	monoclinic	monoclinic	hexagonal
Space group	$P2$	$P2_1$	$P3_12_1$
a [Å]	20.1404(16)	10.9406(6)	10.3614(5)
b [Å]	10.6101(8)	10.0838(6)	10.3614(5)
c [Å]	23.5026(17)	15.7813(9)	31.280(2)
α [°]	90	90	90
β [°]	93.399(2)	104.201(6)	90
γ [°]	90	90	120
Volume /Å^3	5013.5(7)	1687.83	2908.2(3)
Z	4	2	3
D_c [g/cm^3]	1.918	2.022	1.918
Abs. coeff. [mm^{-1}]	5.622	6.249	5.449
F(000)	2776	992	1638
Crystal size [mm]	0.56 × 0.32 × 0.20	0.36 × 0.30 × 0.18	0.36 × 0.30 × 0.18
θ range for data collection	0.87–25.50	2.27–25.49	2.27–25.50
Reflections collected	111275	9901	5869
Independent reflections	18686 [R(int) = 0.041]	5770 [R(int) = 0.032]	3244 [R(int) = 0.055]
Completeness to θ = 25.50°	99.9%	99.8%	92.9%
Refinement method		Full matrix least-squares on F^2	
Data/restraints/parameters	18686/103/1213	5770/1/361	3244/42/233
Goodness-of-fit on F^2	1.106	0.809	0.911
Final R indices	R_1 = 0.0292,	R_1 = 0.0316,	R_1 = 0.0481,
[$I > 2\sigma(I)$]	wR_2 = 0.0703	wR_2 = 0.0546	wR_2 = 0.0831
R indices	R_1 = 0.0318,	R_1 = 0.0464,	R_1 = 0.0696,
(all data)	wR_2 = 0.0717	wR_2 = 0.0563	wR_2 = 0.0879
Largest diff. peak and hole [e·Å^{-3}]	1.275 and –1.505	0.635 and –0.602	0.839 and –0.819

[a] The data for **3b** are given in the Supporting Information (Figure S3).

***spiro*-[MeN(CH_2CMe_2O){(*S*)-CH(Me)-(*R*)-CH(Ph)O}]$_2$Sn (3):** Tetra-*tert*-butoxytin (2.53 g, 6.14 mmol) was dissolved in toluene and a solution of 1 (2.88 g, 1.98 equiv., 12.13 mmol) in toluene was added dropwise over a period of 15 min. The reaction mixture was heated to reflux for two hours and the toluene/*tert*-butanol azeotrope was removed by distillation. Colourless crystals of **3a** (3.11 g, 5.28 mmol, 86%, m.p. 114 °C) were obtained by recrystallization from THF, whereas recrystallization from toluene gave crystals of **3b**. The crystals **3a** and **3b** are different modifications of the same compound. ^{1}H NMR (400.13 MHz, C_6D_6): δ 7.38–7.21 (m, 10 H, H_{arom}), 5.25 [d, $^3J(^1H–^1H)$ = 2 Hz, 2 H, $PhC\mathit{H}O$], 2.67 [d, $^2J(^1H–^1H)$ = 13 Hz, 2 H, $NC\mathit{H}H$] 2.55 (s, 6 H, NCH_3), 2.43 (m, 2 H, $NC\mathit{H}CH_3$), 2.35 [d, $^2J(^1H–^1H)$ = 13 Hz, 2 H, $NCH\mathit{H}$], 1.72 [s, 6 H, $C(CH_3)_2$], 1.38 [s, 6 H, $C(CH_3)_2$], 0.69 [d, 6 H, $^3J(^1H–^1H)$ = 7 Hz, $NCHC\mathit{H}_3$] ppm. $^{13}C\{^1H\}$ NMR (100.63 MHz, C_6D_6): δ 144.7 (C_i), 129.0 (C_o), 128.2 (C_p), 126.4 (C_m), 71.2 (Ph*C*H), 71.0 (N*C*H), 78.1 [$\mathit{C}(CH_3)_2$], 66.9 (NCH_2), 45.0 (NCH_3), 32.0, 30.2 [$C(\mathit{C}H_3)_2$], 10.6 ($NCH\mathit{C}H_3$) ppm. $^{119}Sn\{^1H\}$ NMR (111.89 MHz, C_6D_6): δ –449 ppm. ^{119}Sn CP–MAS NMR (**3b**, 149.22 MHz): δ –449, –452. LC ESI MS (*m*/*z*): calculated for $C_{28}H_{42}N_2O_4Sn$ 590.2, found 591.3 $[C_{28}H_{42}N_2O_4Sn + H^+]^+$. $C_{28}H_{42}N_2O_4Sn$ (589.02): calcd. 57.1, H 7.2, N 4.75, found C 56.9, H 7.2, N 4.7.

[MeN(CH$_2$CMe$_2$O){(*S*)-CH(Me)-(*R*)-CH(Ph)O}SnW(CO)$_5$]$_2$ (4): $W(CO)_6$ (1.84 g, 5.24 mmol) was dissolved in dry THF (250 mL) and exposed to UV irradiation (Hg high pressure lamp, 150 W) to form $W(CO)_5{\cdot}THF$. The progress of the reaction was monitored by the evolution of CO and the reaction was terminated after 110 mL of CO had been formed (theoretically 126 mL). The yellow solution was added dropwise to a solution of **2** (2.09 g, 2.62 mmol) in dry THF (50 mL). The reaction was allowed to complete over a period of 16 h. Evaporation of the solvent and recrystallization from toluene provided colourless crystals of **4**, as its toluene solvate **4**·C_7H_8 (3.22 g, 85%, m.p. 193 °C). ^{1}H NMR (300.13 MHz, CD_2Cl_2): **4**: δ 7.48–7.12 (m, 10 H, $H_{aromatic}$), 5.25 (d, 1 H, $C\mathit{H}Ph$), 3.13 (m, 1 H, $NCH–\mathit{H}_a$), 2.84 (m, 1 H, $C\mathit{H}CH_3$), 2.63 (s, NCH_3), 2.60 (m, 1 H, $NCH–\mathit{H}_b$), 1.96 (s, 3 H, $CC\mathit{H}_3$), 1.62 (s, 3 H, $CC\mathit{H}_3$), 0.82 (m, 3 H, $CC\mathit{H}_3$). ^{1}H NMR (300.13 MHz, CD_2Cl_2): **4a**: δ 7.48–7.12 (m, 10 H, $H_{aromatic}$), 5.93 (m, 1 H, $C\mathit{H}Ph$), 4.10 (m, 1 H, $C\mathit{H}CH_3$), 2.94 (m, 1 H, $NCH–H_a$), 2.37 (d, 1 H, $NCH–H_b$), 1.98 (s, NCH_3), 1.42 (s, 3 H, CCH_3), 1.34 (s, 3 H, CH_3), 1.26 (m, 3 H, $CHC\mathit{H}_3$). $^{13}C\{^1H\}$ NMR (100.63 MHz, CD_2Cl_2) **4**: δ 198.3 ($WCO_{equatorial}$), 197.0 (WCO_{axial}), 143.5 (Ph–C_i), 128.9–125.2 (Ph–C_p, Ph–C_m, Ph–C_o), 74.7 (NCH_2), 68.9 (*C*HPh), 43.4 (NCH_3), 33.7 (CCH_3), 21.0 (CCH_3), 10.3 (CCH_3). $^{13}C\{^1H\}$ NMR (100.63 MHz, CD_2Cl_2) **4a**: δ 198.3 ($WCO_{equatorial}$), 197.0 (WCO_{axial}), 143.5 (Ph–C_i), 128.9–125.2 (Ph–C_p, Ph–C_m, Ph–C_o), 74.6 (NCH_2), 68.0 (*C*HPh), 43.4 (NCH_3), 33.7 (CCH_3), 31.0 (CCH_3), 30.1 (CCH_3), 7.9 (CCH_3) ppm. $^{119}Sn\{^1H\}$ NMR (111.9 MHz, CD_2Cl_2) **4**: δ = –198 [$^1J(^{119}Sn–^{183}W)$ = 1576 Hz], **4a**: –169 [$^1J(^{119}Sn–^{183}W)$ = 1493 Hz]. ^{119}Sn CP–MAS NMR δ = –165, –171, –178 ppm; Intensity: 2:1:1. $C_{38}H_{42}N_2O_{14}Sn_2W_2{\cdot}C_7H_8$ (1447.98): Calcd. C 37.3, H 3.5, N 1.9; found C 37.5, H 3.5, N 1.9. LC ESI MS: Calculated for $[C_{38}H_{42}N_2O_{14}Sn_2W_2 + Na^+]^+$ 1378.0, found $[C_{38}H_{42}N_2O_{14}Sn_2W_2 + Na^+]^+$ 1378.2.

[MeN(CH$_2$CMe$_2$O){(*S*)-CH(Me)-(*R*)-CH(Ph)O}SnBr$_2$]$_2$ (5): Compound **2** (1.60 g, 2.00 mmol) was dissolved in toluene (50 mL) and two molar equivalents (0.64 g, 4.00 mmol, 4.4 mL from a 0.9 M bromine solution in CH_2Cl_2) were added dropwise to the solution. The reaction mixture was heated to reflux and filtered while hot. Slow cooling of the filtrate gave colourless crystals [1.21 g, 59%, m.p. 168 °C (dec.)] suitable for single-crystal X-ray diffraction. Compound **5** is poorly soluble in organic solvents. Consequently, NMR spectra in solution were not recorded. ^{119}Sn CP–MAS NMR (149.23 MHz): δ –503. $C_{28}H_{42}Br_4N_2O_4Sn_2$ (1027.7): calcd. C 32.7, H 4.1, N 2.7; found C 33.1, H 4.4, N 2.6.

[MeN(CH$_2$CMe$_2$O){(*S*)-CH(Me)-(*R*)-CH(Ph)O}]$_2$Sn·SnBr$_4$ (6): After the mother liquor from compound **5** had been stored for several days in sunlight, slightly red crystals separated. X-ray diffraction studies identified these as **6**·C_7H_8. By rational synthesis, **6** was also obtained by the reaction of **3** with tin tetrabromide. Compound **3** (0.98 g, 1.66 mmol) was dissolved in toluene and one molar equivalent (0.73 g, 1.66 mmol) of tin tertabromide dissolved in CH_2Cl_2 (ca. 40 mL) was added dropwise. The reaction mixture was heated to reflux for 10 min. Slow cooling of the solution to room temperature gave colourless crystals of **6**·C_7H_8 [1.41 g, 83%, m.p. 176 °C (dec.)] suitable for single-crystal X-ray diffraction measurements. The crystals were poorly soluble in organic solvents. NMR spectra in solution were not recorded. ^{119}Sn CP–MAS NMR (149.23 MHz): δ = –506 [Sn(1)], –1404 [Sn(2)]. $C_{28}H_{42}Br_4N_2O_4Sn_2{\cdot}C_7H_8$ (1119.8): calcd. C 37.5, H 4.5, N 2.5; found C 37.9, H 3.4, N 2.3.

Bis(tetraphenylphosphonium) Hexabromidostannate (7): Compound **5** (0.115 g, 0.112 mmol) and Ph_4PBr (0.094 g, 0.224 mmol) were mixed in CH_2Cl_2 and stirred for 1 h during which the mixture became a clear solution. The ^{119}Sn NMR spectrum of this solution showed a resonance at δ = –450, which was assigned to **3**. After the solvent had been partially evaporated slowly, yellow crystals separated from the solution. Single crystal X-ray diffraction analysis identified these as **7**. The crystals were isolated by filtration. The filtrate was allowed to stand for several days at room temperature during which crystals of **3** were also formed. ^{1}H NMR (400.13 MHz, $CDCl_3/CD_3CN$): δ 7.91–7.87 (complex pattern, 1 H, H_p), 7.80–7.75 (complex pattern, 2 H, H_m), 7.63–7.58 (complex pattern, H_o) ppm. $^{13}C\{^1H\}$ NMR (100.63 MHz, $CDCl_3/CD_3CN$): δ 135.8 [d, $^4J(^{13}C–^{31}P)$ = 2.9 Hz, C_p], 134.3 [d, $^3J(^{13}C–^{31}P)$ = 10.5 Hz, C_m], 130.8 [d, $^2J(^{13}C–^{31}P)$ = 12.8 Hz, C_o], 117.3 [d, $^1J(^{13}C–^{31}P)$ = 89.6 Hz, C_i] ppm. $^{119}Sn\{^1H\}$ NMR (111.9 MHz, $CDCl_3/CD_3CN$): No signal was observed in the range $2000 < \delta < –2000$ at room temperature. $^{31}P\{^1H\}$ NMR (59.63 MHz, $CDCl_3/CD_3CN$): δ 23.6 ppm. $C_{48}H_{40}Br_6P_2Sn$ (1276.9): calcd. C 45.2, H 3.2; found C 45.4, H 3.1.

MeN(CH$_2$CMe$_2$O)[(*S*)-CH(Me)-(*R*)-CH(Ph)O]Sn[OC(O)Ph]$_2$ (8): Compound **2a** (4.17 g, 5.21 mmol) was dissolved in toluene (100 mL) and dibenzoyl peroxide (2.53 g, 10.40 mmol), which had been dried for 24 h with P_2O_5, was added. The reaction mixture was stirred for 24 h at room temperature and then heated to reflux. The hot reaction mixture was filtered and the filtrate was cooled to room temperature. Compound **8** was isolated as a colourless, amorphous solid [4.01 g, 84%, m.p. 104 °C (dec.)]. ^{1}H NMR (300.13 MHz, C_6D_6): δ 8.40–7.00 (m, 20 H, H_{ar}), 5.34 (m, 1 H, $PhC\mathit{H}O$), 3.58 (m, 1 H, $C\mathit{H}CH_3$), 2.93 (m, 1 H, $NC\mathit{H}_2$), 2.32 [s, $^3J(^1H–^{119}Sn)$ = 30 Hz, 3 H, NCH_3], 2.28 (m, 1 H, $NC\mathit{H}_2$), 1.45 (s, 3 H, $OCC\mathit{H}_3$), 1.38 (s, 3 H, $OCCH_3$), 0.91 (s, 3 H, $NCHC\mathit{H}_3$) ppm. $^{13}C\{^1H\}$ NMR (100.63 MHz, C_6D_6): δ 172.0 [$O\mathit{C}(O)$], 142.3 ($PhC_{i(ephedrine)}$), 134.3, 131.8, 130.3, 128.5, 128.3, 127.5, 126.4 (C_{ar}), 71.8 (O*C*HPh), 68.9 (N*C*HCH$_3$), 68.4 [$\mathit{C}(CH_3)_2$], 65.5 (s, NCH_2), 42.5 (s, N*C*H$_3$), 28.5 (C*C*H$_3$), 27.9 (C*C*H$_3$), 5.0 (NCH*C*H$_3$) ppm. $^{119}Sn\{^1H\}$ NMR (111.9 MHz, C_6D_6): δ = –565 ppm. $C_{28}H_{31}NO_6Sn$ (596.3): calcd. C 56.4, H 5.2, N 2.4; found C 56.6, H 5.2, N 2.2.

Acknowledgments

We thank Dr. Sonja Herres-Pawlis and Dr. Janna Börner for the preliminary studies on the catalytic activity towards lactide polymerization.

---

[1] a) A. A. Selina, S. S. Karlov, E. K. Lermontova, G. S. Zaitseva, *Chem. Heterocycl. Compd.* **2007**, *43*, 813–834; b) N. Hollingsworth, G. A. Horley, M. Mazhar, M. F. Mahon, K. C. Molloy,

P. W. Haycock, C. P. Myers, G. W. Critchlow, *Appl. Organomet. Chem.* **2006**, *20*, 687–695; c) N. N. Zemlyanski, I. V. Borisova, M. G. Kuznetsova, V. N. Khrustalev, Y. A. Ustynyuk, M. S. Nechaev, V. V. Lunin, J. Barrau, G. Rima, *Organometallics* **2003**, *22*, 1675–1681; d) V. N. Khrustalev, I. A. Portnyagin, N. N. Zemlyansky, I. V. Borisova, Y. A. Ustynyuk, M. Y. Antipin, *J. Organomet. Chem.* **2005**, *690*, 1056–1062; e) V. N. Khrustalev, I. A. Portnyagin, N. N. Zemlyansky, I. V. Borisova, M. S. Necheav, Y. A. Ustynyuk, M. Y. Antipin, *J. Organomet. Chem.* **2005**, *690*, 1172–1177; f) V. N. Khrustalev, N. N. Zemlyansky, I. V. Borisova, M. G. Kuznetsova, E. B. Krut′ko, M. Y. Antipin, *Russ. Chem. Bulletin, Int. Ed.* **2007**, *56*, 267–270; g) I. A. Portnyagin, M. S. Nechaev, V. N. Khrustalev, N. N. Zemlyansky, I. V. Borisova, M. Y. Antipin, Y. A. Ustynyuk, V. V. Lunin, *Eur. J. Inorg. Chem.* **2006**, 4271–4277; h) O. V. Chernov, A. Yu. Smirnov, I. A. Portnyagin, V. N. Khrustalev, M. S. Nechaev, *J. Organomet. Chem.* **2009**, *694*, 3184–3189; i) I. A. Portnyagin, M. S. Nechaev, *J. Organomet. Chem.* **2009**, *694*, 3149–3153; j) M. Huang, E. K. Lermontova, K. V. Zaitsev, A. V. Churakov, Y. F. Oprunenko, J. A. K. Howard, S. S. Karlov, G. S. Zaitseva, *J. Organomet. Chem.* **2009**, *694*, 3828–3832.

[2] J. Krause, S. Reiter, S. Lindner, A. Schmidt, K. Jurkschat, M. Schürmann, G. Bradtmöller, DE 10 2008 021 980A1, **2009**.

[3] a) N. Nimitsirivat, V. C. Gibson, E. L. Marshall, M. R. J. Elsegood, *Dalton Trans.* **2009**, 3710–3715; b) M. H. Chisholm, E. E. Delbridge, *New J. Chem.* **2003**, *27*, 1177–1183; c) M. H. Chisholm, E. E. Delbridge, *New J. Chem.* **2003**, *27*, 1167–1176; d) M. H. Chisholm, E. E. Delbridge, J. C. Galluci, *New J. Chem.* **2004**, *28*, 145–152.

[4] R. Contreras, A. Flores-Parra, H. C. López-Sandoval, N. Barba-Behrens, *Coord. Chem. Rev.* **2007**, *251*, 1852–1867.

[5] V. M. Jiménez-Pérez, H. Nöth, A. Ariza-Castolo, A. Flores-Parra, R. Contreras, *J. Organomet. Chem.* **2006**, *691*, 1584–1589.

[6] a) A. Zschunke, C. Mügge, M. Scheer, K. Jurkschat, A. Tzschach, *J. Crystallogr. Spectrosc. Res.* **1983**, *13*, 201–210; b) A. Tzschach, K. Jurkschat, M. Scheer, J. Meunier-Piret, M. Van Meerssche, *J. Organomet. Chem.* **1983**, *259*, 165–170; c) T. Berends, L. Iovkova, G. Bradtmöller, I. Oppel, M. Schürmann, K. Jurkschat, *Z. Anorg. Allg. Chem.* **2009**, *635*, 369–374; d) T. Zöller, L. Iovkova-Berends, C. Dietz, T. Berends, K. Jurkschat, *Chem. Eur. J.* **2011**, *17*, 2361–2364.

[7] R. Colton, D. Dakternieks, *Inorg. Chim. Acta* **1983**, *71*, 101–107.

[8] R. H. Al-Far, S. F. Haddad, B. F. Ali, *Acta Crystallogr., Sect. E* **2009**, *65*, m583–m584.

[9] G. M. Sheldrick, *Acta Crystallogr., Sect. A* **1990**, *46*, 467.

[10] G. M. Scheldrick, University of Göttingen, **1997**.

[11] *International Tables for Crystallography*, **1992**, vol. C, Kluwer Academic Publishers, Dordrecht, The Netherlands.

[12] A. L. Spek, *Acta Crystallogr., Sect. D* **2009**, *65*, 148–155.

[13] G. M. Sheldrick, **1997**, *SHELXTL*. Release 5.1 Software Reference Manual, Bruker AXS, Inc., Madison, Wisconsin, USA.

[14] K. V. Zaitsev, M. V. Bermeshev, A. A. Samsonov, J. F. Oprunenko, A. V. Churakov, J. A. L. Howard, S. S. Karlov, G. S. Zaitseva, *New J. Chem.* **2008**, *32*, 1415–1431.

Received: April 1, 2011